

Egyptian Journal of Chemistry

http://ejchem.journals.ekb.eg/



Electrochemical Study of Uranyl-Paracetamol Interactions in Solution: Cyclic Voltammetry and Molecular Docking Approaches



Hadwah A. Kamal El-din ^{1, 2}, Safa Q. Hussien ³, Ibrahim E. Mohi El-Din ¹, Tarek A. Mohsen ⁴, Esam A. Gomaa ³, Elsayed M. AbouElleef ^{5*}

- ¹ Chemistry Department, Faculty of Science, Port Said University, Port Said, Egypt.
- ² Department of Medical Analysis, Ophthalmology Center, Mansoura University, Mansoura, Egypt.
- ³ Chemistry Department, Faculty of Science, Mansoura University, Mansoura, Egypt.
- ⁴Ophthalmology Department, Faculty of Medicine, Mansoura University, Mansoura, Egypt.
- ⁵Basic Sciences Department, Delta Higher Institute for Engineering and Technology, Mansoura, Egypt.

Abstract

The electrochemical behaviour of paracetamol was investigated in various electrolyte environments, with a focus on its interaction with uranyl ions in alkaline medium. Cyclic voltammetry revealed evidence of complex formation, supported by shifts in peak potentials and increased current responses. Thermodynamic parameters were estimated from electrochemical data, confirming the stability and spontaneity of the complexes. Molecular docking studies with viral (7JWY) and cancer-related (5IXB) proteins were also performed to evaluate theoretical binding affinity. The findings suggest that paracetamol can form stable coordination complexes with uranyl ions and potentially interact with biologically relevant targets.

Keywords: Uranyl nitrate; Solvation parameters; stability constants; Paracetamol; Cyclic voltammetry.

1. Introduction

Paracetamol, also known as acetaminophen, is a widely used analgesic and antipyretic treatment of headaches, fever, and musculoskeletal pain. It is often prescribed following surgical procedures and in the management of osteoarthritis and rheumatoid arthritis. Despite its therapeutic prevalence, the full scope of its molecular interactions remains under investigation [1, 2]. Cyclic voltammetry (CV) is a powerful electrochemical technique for studying redox behaviour in solutions. It offers detailed insights into electron transfer mechanisms and the stability of electroactive species. In alkaline media, uranyl (VI) ions form hydroxo complexes whose formation and electrochemical characteristics can be effectively monitored using CV, particularly at low concentrations where precipitation is absent [3-10]. In basic environments, uranyl ions $(\mathrm{UO}_2^{2^+})$ sequentially react with hydroxide ions to form hydroxo complexes such as $\mathrm{UO}_2(\mathrm{OH})^+$, $\mathrm{UO}_2(\mathrm{OH})_2$, $\mathrm{UO}_2(\mathrm{OH})_3^-$, and $\mathrm{UO}_2(\mathrm{OH})_4^{2^-}$ [11, 12]. These reactions are outlined as follows, Equations (1-4):

$$UO_2^{2+}$$
 + $OH^- \leftrightarrow UO_2(OH)^+$ (1)

$$UO_2(OH)^+ + OH^- \leftrightarrow UO_2(OH)_{2(aq)}$$
 (2)

$$UO_2(OH)_{2(aq)} + OH^- \leftrightarrow UO_2(OH)_3^-$$
 (3)

$$UO_2(OH)_3$$
 + OH \leftrightarrow $UO_2(OH)_4$ ² (4)

Nuclear magnetic resonance (NMR) and density functional theory (DFT) analyses confirm that $UO_2(OH)_4^{2^-}$ is a dominant binuclear hydroxo complex of uranyl(VI) in strong alkaline conditions [13].

In alkaline media, paracetamol undergoes deprotonation to form anionic species, which enhances its solubility and reactivity. These negatively charged molecules interact electrostatically with uranyl ions, promoting the formation of stable soluble complexes. This interaction is of interest for its potential role in heavy metal detoxification and extraction [14].

In sodium hydroxide (NaOH) solutions, paracetamol facilitates uranyl ion stabilization by preventing precipitation, leading to the formation of soluble uranyl-paracetamol complexes. UV-Vis spectrophotometry was used to monitor the formation kinetics and calculate Gibbs free energy (Δ G), indicating that increased alkalinity enhances the rate of complex formation. These findings point to potential applications in uranium recovery processes, such as the extraction of uranium from radioactive waste. Paracetamol may serve as a viable alternative to conventional chelating agents.

Additionally, its stabilizing effect could support the production of sodium uranate, a yellow pigment used in ceramics. Tailoring paracetamol derivatives could further improve binding affinity and extraction efficiency [15].

*Corresponding author e-mail s.abouelleef@mail.com.; (Elsayed M. AbouElleef). Received date 24 May 2025; Revised date 14 July 2025; Accepted date 03 August 2025 DOI: 10.21608/EJCHEM.2025.388651.11815

© 2026 National Information and Documentation Center (NIDOC)

Commercially known as Tylenol, paracetamol exhibits weak acidic behavior and can coordinate with metal ions in alkaline media. This characteristic makes it useful in several applications: Precipitation and extraction of metal ions through pH manipulation [16-19]. Electrochemical sensing of metal ions, with paracetamol acting as a ligand [20-23].

Novelty of the Work:

Unlike previous studies that primarily focused on spectroscopic or theoretical evaluations, the present work provides novel insights into the redox behaviour and complexation dynamics between paracetamol and uranyl ions using cyclic voltammetry in alkaline media a system not previously explored in this context. The study introduces a quantitative electrochemical approach to assess the stability and formation of uranyl–paracetamol complexes, supported by kinetic and thermodynamic parameters. Furthermore, it incorporates molecular docking simulations with biologically relevant proteins (7JWY and 5IXB) to explore the theoretical biomedical relevance of paracetamol–metal interactions. This integrated electrochemical–theoretical strategy adds a new dimension to the understanding of ligand–actinide behaviour and opens avenues for future applications in bioinorganic, environmental, and analytical chemistry.

2. Materials and Methods

2.1 Chemicals and Instrumentation

All solutions were prepared using high-purity deionized water. Analytical-grade reagents were procured from Sigma-Aldrich and used without further purification. These included uranyl nitrate hexahydrate (UO_2 (NO_3)₂ ·6H₂ O), paracetamol (C_8 H₉ NO_2), potassium bromide (KBr), hydrochloric acid (HCl, 0.1 M), and sodium hydroxide (NaOH, 0.1 M).

Electrochemical measurements were performed using a DY 2000 potentiostat (USA), equipped with a conventional three-electrode system. The working electrode was a glassy carbon electrode (GCE), selected for its wide electrochemical window and chemical stability. A saturated calomel electrode (SCE) served as the reference electrode, and a platinum wire functioned as the counter electrode. All experiments were conducted at a controlled temperature of 298.15 K. The potential window for cyclic voltammetry (CV) measurements was set from +1.5 V to -1.5 V. Different scan rates were applied to evaluate the redox kinetics, although the primary scan rate used for comparative analysis was 0.1 V/s [24, 25].

2.2 Cyclic Voltammetry Analysis

The DY 2000 potentiostat was interfaced with a three-electrode electrochemical cell to perform CV studies. Prior to each measurement, solutions were degassed with high-purity nitrogen (N_2) gas for 15 minutes to eliminate dissolved oxygen, thereby avoiding interference from oxygen reduction reactions.

Electrochemical scans were conducted using the following setup:

Working Electrode: Glassy carbon electrode (GCE). Reference Electrode: Saturated calomel electrode (SCE). Counter Electrode: Platinum wire.

All CV experiments were carried out within the potential range of +1.5 V to -1.5 V, with a scan rate of 0.1 V/s unless otherwise specified. This configuration ensured reproducibility and sensitivity for redox behavior assessment.

2.3 Experimental Procedure

Stock solutions of paracetamol (0.01 M) were prepared in four different media: 0.1 M NaOH, KBr, HCl, and KCl. Uranyl nitrate (0.01 M) was dissolved in 0.1 M NaOH for studies involving complexation and redox interactions.

A 30 mL aliquot of each solution was used for electrochemical analysis in the three-electrode cell. CV measurements were conducted under identical experimental conditions for consistency. Each experiment was performed in triplicate to ensure reproducibility and reliability of the data.

Electrochemical parameters such as anodic and cathodic peak potentials (E, a and E, c) and corresponding peak currents (I, a and I, c) were recorded. From the resulting voltammograms, diffusion coefficients and electrochemical stability constants were calculated.

To assess the antioxidant capability of paracetamol, the effect of increasing its concentration on the oxygen reduction wave was systematically evaluated. This provided insights into the electron-donating capacity of paracetamol in different electrolyte environments.

This methodological framework enabled a comprehensive evaluation of the electrochemical behavior of paracetamol, its interaction with uranyl ions, and its role as an antioxidant and potential metal chelator.

3. Results and Discussion

3.1. Redox Behaviour of Paracetamol in Different Electrolytes

Cyclic voltammetry (CV) was employed to investigate the redox characteristics of paracetamol (0.01 M) in different electrolytic media HCl, KCl, NaOH, and KBr using a glassy carbon electrode at 298.15 K and a scan rate of 0.1 V/s. The voltammograms obtained are shown in Fig. 1.

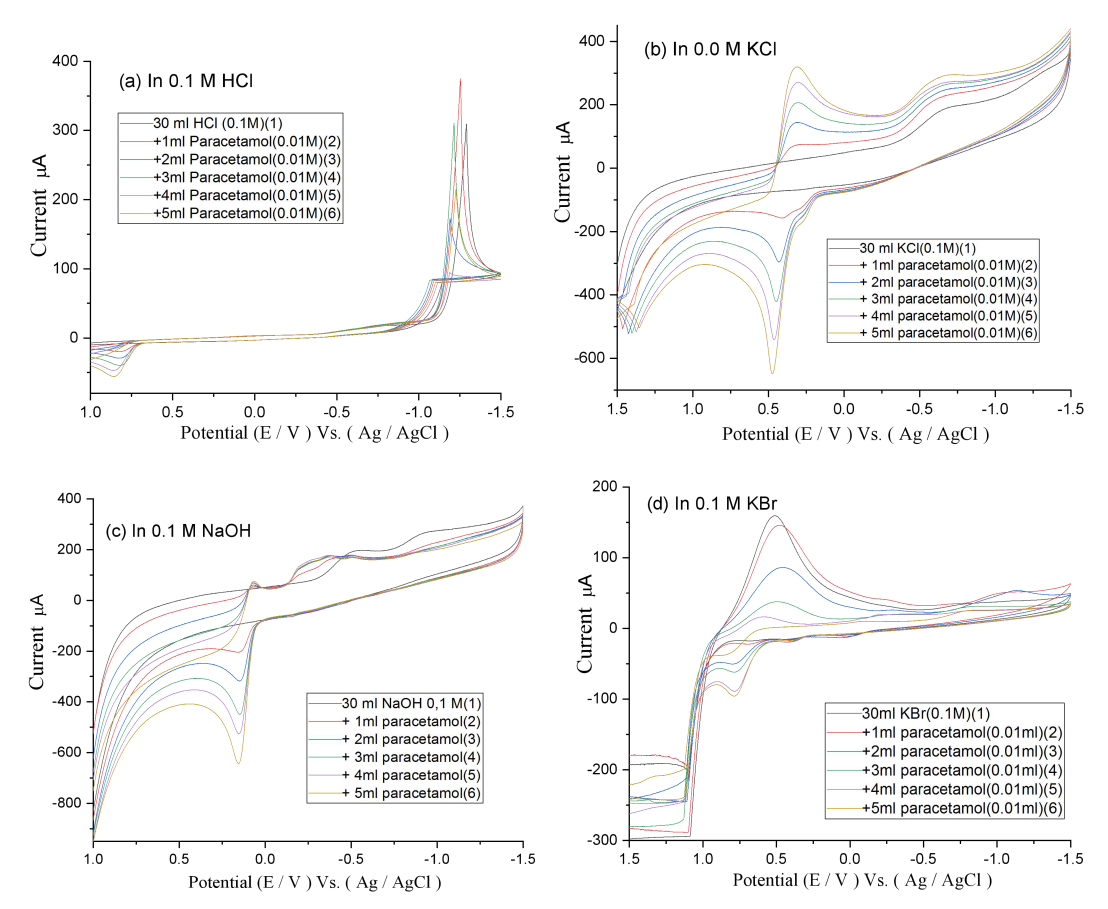


Fig. 1. Redox Behaviour of Paracetamol in Different Electrolytes

Cyclic voltammogram of Paracetamol (0.01 M) in 0.1 M solutions of (a) HCl, (b) KCl, (c) NaOH, and (d) KBr, at 298.15 K using a glassy carbon working electrode, SCE reference electrode, and platinum counter electrode. Scan rate: 0.1 V/s.

The CV profiles revealed the following redox behaviours:

- HCl Medium: A single oxidation peak at 0.8 V was observed without a corresponding reduction peak, indicating
 an irreversible oxidation process.
- KCl Medium: Oxidation and reduction peaks appeared at 0.5 V and 0.25 V, respectively, indicating a moderate redox reaction.
- NaOH Medium: Oxidation occurred at 0.1 V and reduction at 0 V, indicating a facile redox process.
- KBr Medium: A marked suppression of the oxygen wave suggested a strong antioxidant response by paracetamol.

In HCl medium, a single irreversible oxidation peak for paracetamol is observed at approximately +0.80 V vs. Ag/AgCl, without a corresponding cathodic peak, indicating the formation of a radical intermediate such as N-acetyl-p-benzoquinone imine (NAPQI). In alkaline medium (NaOH), both anodic and cathodic peaks are more prominent, and the peak separation (Δ Ep) suggests a quasi-reversible process. The shift of oxidation potential to lower values in alkaline medium indicates facilitated electron transfer due to deprotonation and stabilization of the oxidized species. These changes reflect the influence of the medium on the redox mechanism of paracetamol and point to possible proton-coupled electron transfer (PCET) behaviour.

3.2. Antioxidant Behaviour of Paracetamol in KBr Medium

Table 1 summarizes the CV parameters for varying concentrations of paracetamol in 0.1 M KBr medium.

| [L] | Volt | | | Amp | | <i>I</i> p,a/ <i>I</i> p,c | volt | |
|-----------------------------------|------------------|---------------|---------------|-----------------------------------|-----------------------|----------------------------|----------------------|------------------------|
| mol. L ⁻¹ | (-) <i>E</i> p,a | Ep,c | ∆ <i>E</i> p | (-) <i>I</i> p,a (μ | (-) <i>I</i> p,a (μA) | | 1p,a/1p,c | E ° |
| 1.61 x10 ⁻³ | 0.692 | 0.480 | 0.211 | 5.65 | | 164.0 | 0.034 | 0.586 |
| 3.13 x10 ⁻³ | 0.784 | 0.455 | 0.328 | 33.3 | | 96.2 | 0.346 | 0.619 |
| 4.55 x10 ⁻³ | 0.784 | 0.441 | 0.342 | 41.1 | | 43.8 | 0.938 | 0.612 |
| 5.88 x10 ⁻³ | 0.784 | 0.369 | 0.414 | 66.6 | | 17.4 | 3.834 | 0.576 |
| 7.14 x10 ⁻³ | 0.795 | 0.742 | 0.053 | 75.8 | | 14.8 | 5.110 | 0.768 |
| Dex10 ⁵ | <i>E</i> pc/2 | Epa- | a na € | $k_{\rm sc} \times 10^2$ | Tc x109 mol.cm | (+) Qcx10 ⁵ | Γa x10 ⁹ | (-) Qax10 ⁵ |
| cm ⁻² .s ⁻¹ | | <i>E</i> pc/2 | | cm ⁻² .s ⁻¹ | 2 | columb | mol.cm ⁻² | columb |
| 18.5 | 0.696 | 0.216 | 0.226 | 1.55 | 14.182 | 8.59 | 0.488 | 0.29 |
| 1.70 | 0.702 | 0.247 | 0.197 | 4.13 | 8.326 | 5.04 | 2.882 | 1.75 |
| 0.166 | 0.700 | 0.259 | 0.188 | 1.65 | 3.787 | 2.29 | 3.555 | 2.15 |
| 0.016 | 0.762 | 0.393 | 0.124 | 1.63 | 1.504 | 0.91 | 5.765 | 3.49 |
| 0.008 | 0.787 | 0.044 | 1.083 | 0.341 | 1.283 | 0.78 | 6.557 | 3.97 |

Table 1. Electrochemical parameters for paracetamo (0.01 M) in 30 mL of 0.1 M KBrat 298.15 K, scan rate = 0.1 V/s.

This table summarizes the key electrochemical parameters for paracetamol in 0.1 M KBr, focusing on its antioxidant behaviour. The anodic (Ep,a) and cathodic (Ep,c) peak potentials represent the redox transitions of paracetamol. Their separation (Δ Ep) is an indicator of reversibility; in this case, values >0.059 V suggest quasi-reversible or irreversible behaviour. The corresponding peak currents (Ip,a and Ip,c) reflect the rate of electron transfer. As paracetamol concentration increases, the magnitude of these currents increases, supporting enhanced redox activity and possible antioxidant action through oxygen scavenging.

The formal potential (E°) , calculated as the average of Ep,a and Ep,c, gives insight into the intrinsic redox characteristics of paracetamol. Additional parameters such as the diffusion coefficient (Dc), surface coverage (Γ a and Γ c), and charge passed (Qa and Qc) help evaluate the electroactive surface behaviour. The standard rate constant (ks) and transfer coefficient (α na) provide kinetic information higher values denote faster electron transfer processes. These results collectively support the claim that paracetamol exhibits enhanced electrochemical activity in KBr medium due to its radical scavenging behaviour. As paracetamol concentration increased, the intensity of the oxygen wave diminished, supporting its antioxidant behaviour. Enhanced anodic and cathodic peak currents at higher concentrations reflected improved electron transfer kinetics. The fading oxygen reduction wave indicated effective scavenging of oxygen free radicals.

The redox mechanism for paracetamol is depicted in Eq (5):

Eq. (5): Paracetamol reduction involves hydrogen ion consumption from the aqueous phase and reduction at the oxygen atom.

The pronounced effect of paracetamol on the oxygen wave underscores its potential as an antioxidant. The three-dimensional relationship between paracetamol concentration and oxygen wave parameters is shown in Fig. 2.

Fig. 2: 3D representation showing the suppression of the oxygen wave with increasing paracetamol concentration in KBr medium. The oxygen reduction and oxidation reactions are proposed at about 0.5 V as follows, Eq (6):

$$O_2 + 2H^+ + 2e^- \leftrightarrow H_2O_2$$
 (6)

And oxidation at about 0.7 V with the given suggested mechansim as given in electrochemical series, Eq (7) [26]:

$$2OH^{-} + 2H_{2}O_{2} \leftrightarrow O_{2} + H_{2}O + 2e^{-}$$
 (7)

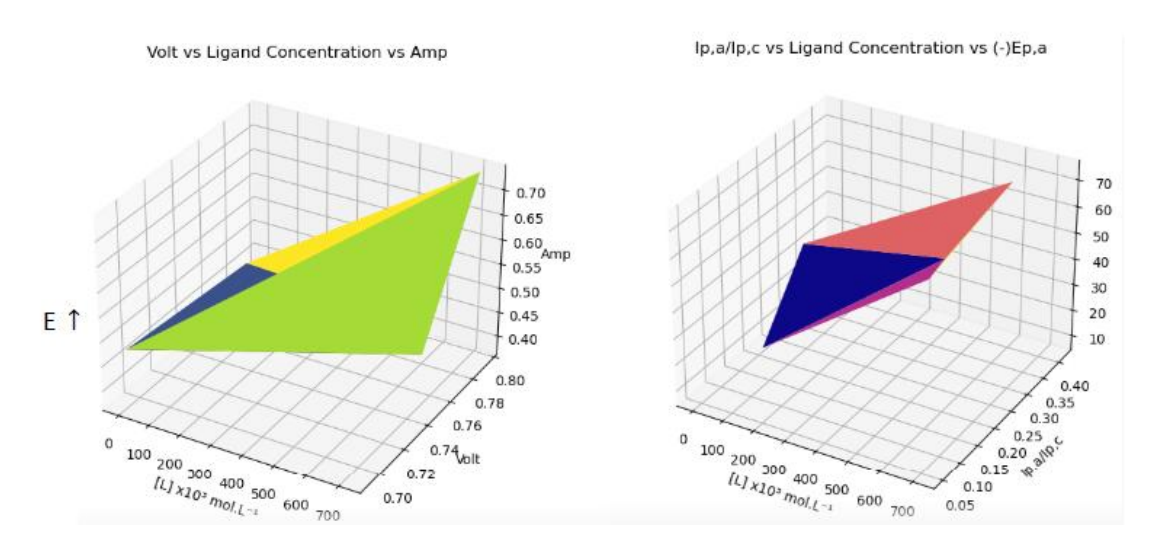


Fig. 2. Antioxidant Activity of Paracetamol in KBr Medium

3D plot showing suppression of the oxygen reduction wave with increasing paracetamol concentrations in 0.1 M KBr medium. The data reflect antioxidant activity through decreasing oxygen wave intensity.

The plot demonstrates the gradual suppression of the oxygen wave with increasing paracetamol concentration, confirming its antioxidant activity. This 3D visualization demonstrates how increasing paracetamol concentration progressively diminishes the oxygen reduction wave (\sim 0.5 V) and oxidation wave (\sim 0.7 V). These reactions support the role of paracetamol as a radical scavenger, as evidenced by the progressive attenuation of the oxygen redox waves.

The observed suppression of the oxygen reduction wave with increasing paracetamol concentration is primarily attributed to a diffusion-controlled process, as evidenced by the linear relationship between peak current (Ip) and the square root of scan rate ($\sqrt{\nu}$), which is characteristic of diffusion-limited electrochemical reactions. While some degree of surface interaction (adsorption) cannot be entirely ruled out, especially at higher concentrations, no significant deviation from the Randles-Ševčík behavior was observed in our data, suggesting that adsorption phenomena play a minor role under the studied conditions.

These findings support the hypothesis that paracetamol acts as an effective electrochemical antioxidant by interacting with oxygen radicals in solution via a diffusion-dominated process, making it a potentially useful ligand for modulating redoxactive environments.

3.3. Redox Behaviour of Uranyl Ions in Alkaline Medium and the Influence of Paracetamol

To investigate the redox properties of uranyl ions and assess the stabilizing effect of paracetamol, cyclic voltammetry experiments were carried out in 0.1 M NaOH containing 0.01 M uranyl nitrate. Fig. 3 illustrates the resulting voltammogram. Within the potential window of +1.5 V to -1.5 V, two distinct reductions and two oxidation peaks were observed, indicating multiple redox transitions involving uranyl hydroxide complexes.

In the absence of paracetamol, the voltammetric response exhibited weak current signals, suggesting limited electrochemical activity of uranyl ions in alkaline medium. The observed redox peaks are attributed to the formation of species such as UO_2 (OH)₅ ³⁻, and UO_3 (OH)₃ ³⁻, consistent with known hydroxo-complexation behaviour under alkaline conditions. The following redox processes are proposed based on the peak positions:

Reduction Reaction (Step 1), Eq (8).:

$$[UO_2(OH)_4]^{2-} + 1/2 H_2O + e_- \leftrightarrow [UO_2(OH)_5]^{3-}$$
 (8)

Oxidation Reaction (Step 2), Eq (9).:

$$[UO_2(OH)_4]^{2-} + e^{-} \rightleftharpoons [UO_3(OH)_3]^{3-} + H^{+}$$
(9)

Effect of Paracetamol:

• The formation of stable paracetamol-uranyl complexes was observed. Enhanced diffusion coefficients and current responses confirm increased stabilization of uranyl species.

Upon addition of paracetamol to the uranyl system, significant changes in the voltammetric profile are observed. New peaks emerge or shift in position, indicating complex formation between paracetamol and the uranyl ion. Specifically, the appearance of two cathodic peaks around -0.65 V and -0.95 V vs. Ag/AgCl is attributed to the stepwise reduction of U(VI) to U(V) and U(V) to U(IV). These processes are further supported by anodic waves that suggest partial reversibility, depending on paracetamol concentration.

The negative shift in reduction potential and the increase in peak current upon increasing ligand concentration confirm complexation and stabilization of reduced uranium species. These observations are consistent with a ligand-mediated electron transfer mechanism, where paracetamol facilitates reduction by forming more stable intermediate species. The interaction alters the redox potential and enhances the electrochemical activity, confirming the formation of a uranyl–paracetamol complex.

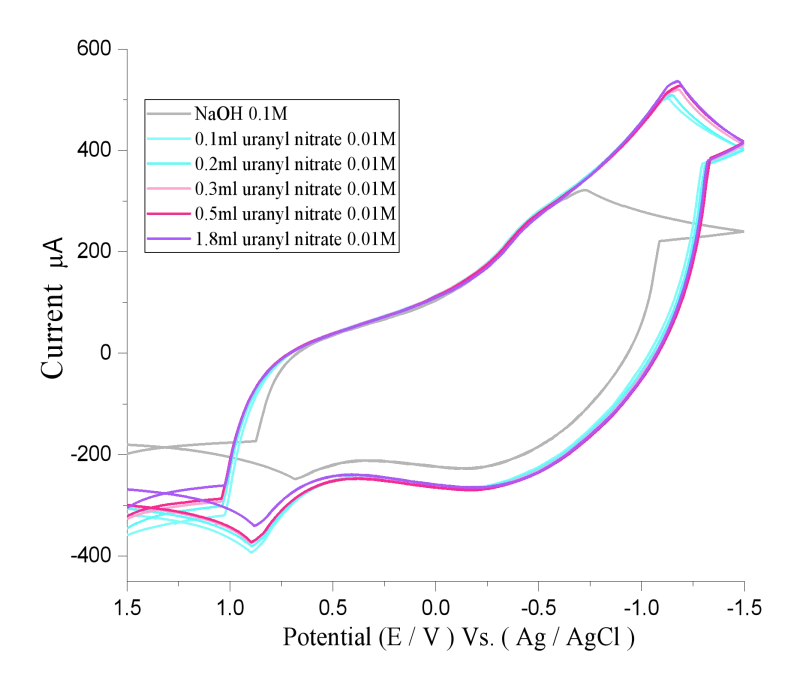


Fig. 3. CV of Uranyl Ions in NaOH (Without Paracetamol)

Cyclic voltammogram of uranyl nitrate (0.01 M) in 0.1 M NaOH at 298.15 K. Peaks correspond to redox processes involving uranyl hydroxyl complexes. Scan rate: 0.1 V/s.

The introduction of paracetamol to the uranyl nitrate system in 0.1 M NaOH significantly altered the voltammetric profile (Fig. 4). Enhanced redox peaks were recorded, accompanied by increased peak currents and diffusion coefficients, as shown in Tables 2 and 3. These changes suggest the formation of electroactive and more soluble uranyl–paracetamol complexes, indicating that paracetamol serves as a stabilizing ligand.

Under identical electrochemical conditions (scan rate: $0.1~\rm V\cdot s^{-1}$; temperature: 298.15 K), the presence of paracetamol shifted the redox potentials and amplified both anodic and cathodic responses. The interaction window remained between approximately $+1.0~\rm V$ and $-1.5~\rm V$. Two reductions and two oxidation processes were consistently observed, supporting the existence of complex multi-step electron transfer pathways. According to literature and DFT calculations, the redox mechanism likely involves oxygen exchange through hydroxyl coordination, as described below [27]:

Revised Reduction Step (with paracetamol), Eq. (10):

$$[UO_2(OH)_4]^{2-} + 1/2 H_2(H_2O) + e- \leftrightarrow [UO_2(OH)_5]^{3-}$$
(10)

The suggested mechanism for the second oxidation with its reverse oxidation process is represented as suggested from DFT calculations in literature [11] is given in equation (5).

The examination of waves was carried out in accordance with earlier research. Four peaks in each phase indicate an increase in uranyl nitrate reduction and oxidation, indicating that complexion was completed and displayed in Fig. 4.

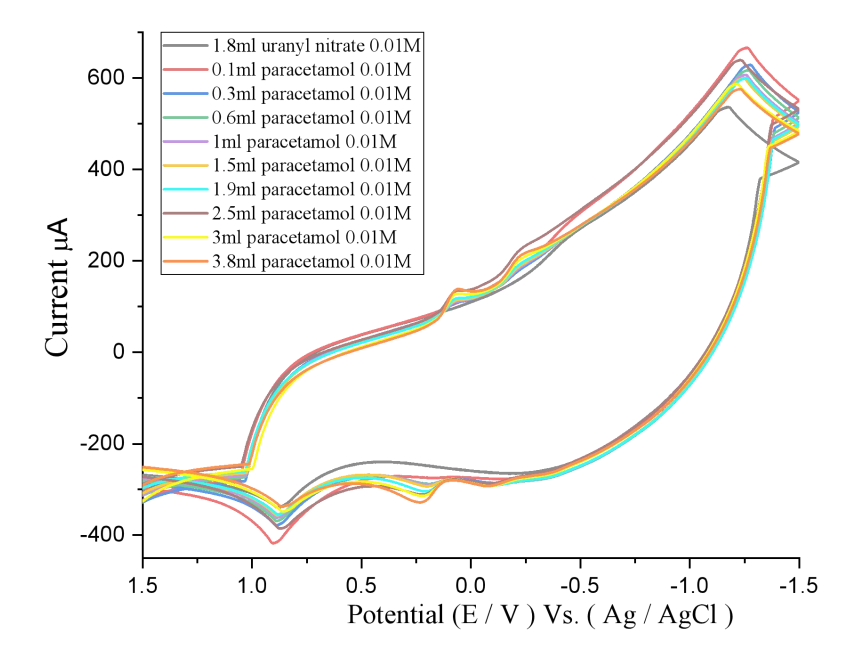


Fig. 4. CV of Uranyl Ions in NaOH with Paracetamol

Cyclic voltammogram of uranyl nitrate (0.01 M) with paracetamol (0.01 M) in 0.1 M NaOH at 298.15 K. Enhanced peak currents indicate the formation of uranyl–paracetamol complexes. Scan rate: 0.1 V/s.

The enhanced peaks confirm the formation of stable uranyl-paracetamol complexes. Enhanced peak currents and diffusion coefficients (Tables 2–3) confirm paracetamol stabilizes uranyl ions, forming soluble complexes. The redox mechanism follows Eq. 6, where paracetamol acts as a chelating ligand for UO_2^{2+} .

The waves seen in Fig. 4 correspond to the redox reaction of uranyl hydroxyl complexes because it is increased by increase uranyl ion concentration and the waves lie in different potentials for that of paracetamol.

The general redox equation for the UO_2^{2+} and paracetamol reactions increased, Eq (11) [11–12].

Paracetamol-Assisted Complex Formation

$$UO_2^{2+} + paracetamol \rightarrow UO_2^2(paracetamol)^{2+} + e$$
 (11)

These findings confirm the enhanced redox activity and complexation of U(VI) species in the presence of paracetamol. The increases in both anodic and cathodic charges (Q_a , Q_c), as well as the surface coverage (Γ_a , Γ_c), suggest that paracetamol facilitates a more efficient electron transfer by stabilizing uranyl ions through chelation.

Tables 2 and 3 provide detailed electrochemical parameters corresponding to the first (U^6) and second (U^4) redox transitions, respectively. Notably, the peak separation (ΔE_P), standard rate constants (K_S), and diffusion coefficients (D_a , D_c) demonstrate a concentration-dependent effect, supporting the hypothesis of complex formation. For instance, increasing paracetamol concentration led to enhanced peak currents and more pronounced reversibility in the redox cycles.

Table 2 outlines the electrochemical behaviour of the first redox couple, associated with the U(VI)/U(V) transition. The anodic (Ep,a) and cathodic (Ep,c) peak potentials shift with increasing paracetamol concentration, indicating progressive complexation and alteration of uranyl's redox environment. The increasing peak currents (Ip,a and Ip,c) suggest more electroactive species are formed as paracetamol binds uranyl ions, supporting the formation of soluble uranyl–paracetamol complexes.

Table 2. Electrochemical Parameters for the First Redox Wave (U 6 $^{+}$). Conditions: 0.01 M Paracetamol, 298.15 K, 0.1 V·s $^{-}$ $^{-1}$, 0.1 M NaOH

| [L] | volt | | | | amp | | <i>Ip</i> ,a/ <i>I</i> p,c | volt | |
|--|--|--------|-------------------------------|----------------------|---------|--------------------------------------|----------------------------|--|--------------------------------------|
| mol.L ⁻¹ | <i>E</i> p,a | Ep,c | | ΔE p | | (-) <i>I</i> p,a (μΑ | .) <i>I</i> p,c (μA) | | E ° |
| 9.35 x10 ⁻³ | 0.4204 | 0.0972 | | 0.5177 | | 10.3 | 24.2 | 4.2504 | 0.1615 |
| 1.85 x10 ⁻³ | 0.2573 | 0.0877 | | 0.3450 | | 10.5 | 39.1 | 0.2698 | 0.0848 |
| 5.64 x10 ⁻³ | 0.3418 | 0.0869 | | 0.4288 | 70.6 | | 39.5 | 1.7867 | 0.1274 |
| 7.29 x10 ⁻³ | 0.3961 | 0.0928 | | 0.4889 | | 71.2 | 62.2 | 1.4796 | 0.1516 |
| 1.07 x10 ⁻³ | 0.3583 | 0.0960 | | 0.4544 | | 93.8 | 63.4 | 1.1442 | 0.1311 |
| Da x10 ⁵ cm ² .s ⁻¹ | Dc x10 ⁵ cm ² .s ⁻¹ | Epc/2 | <i>E</i> pa- <i>E</i> pc/2 | $K_{\rm s}$ x 10^2 | Го m | x10 ⁹ ol.cm ⁻² | (+) Qcx10 ⁵ C | Γa x10 ⁹ mol.cm ⁻² | (-) <i>Q</i> a x10 ⁵ C |
| 4.64 | 1.19 | 0.1457 | 0.0484 | 1.86 | 2.2 | 2369 | 4.07 | 9.5078 | 1.73 |
| 3.21 | 3.15 | 0.1441 | 0.0564 | 8.25 | 3.0 | 6071 | 6.56 | 6.5169 | 1.18 |
| 4.98 | 3.49 | 0.1115 | 0.0245 | 8.96 | 3.0 | 6473 | 6.63 | 9.7342 | 1.77 |
| 4.51 | 9.30 | 0.1366 | 0.0438 | 3.04 | 5. | 7420 | 1.04 | 8.6607 | 1.57 |
| 3.55 | 9.65 | 0.1265 | 0.0305 | 2.91 | 5. | 7420 | 1.04 | 6.5703 | 1.19 |

The diffusion coefficients (Da and Dc) increase with ligand concentration, indicating enhanced ion mobility due to stabilization of soluble complexes. The peak separation (Δ Ep) values and the formal potential (E°) show that the redox reaction becomes more favorable in the presence of paracetamol. The standard rate constants (ks) and transfer coefficients (α na) further confirm faster kinetics and greater electrochemical reversibility. Additionally, the increase in surface coverage (Γ a and Γ c) and charge passed (Qa and Qc) validates the increased electron flow and adsorptive behavior of the complex. These observations affirm that paracetamol enhances the redox activity of U(VI) species by acting as a chelating ligand. The electrochemical parameters for the second redox wave (U^{*}) of uranyl-paracetamol interactions are summarized in Table 3, showing the influence of paracetamol concentration on peak potentials, currents, and derived thermodynamic quantities (e.g., diffusion coefficients, charge transfer).

Table 3. Electrochemical Parameters for the Second Redox Wave (U^{4+}). Conditions: 0.01 M Paracetamol, 298.15 K, 0.1 V·s⁻¹, 0.1 M NaOH

| [L] | Volt | Volt | | | | | | <i>I</i> p,a/ <i>I</i> p,c | Volt |
|--|--|---------------|-------------------------------|---------------------|--|------|----------------------|--|-----------------------------------|
| mol.L ⁻¹ | <i>E</i> p,a | Ep,c | | ΔE p | (-) <i>I</i> p,a (μA) | | <i>I</i> p,c (μA) | | E ° |
| 9.35 x10 ⁻³ | 0.1357 | 0.2103 | | 0.0746 | 51.1 | | 65.8 | 0.7775 | 0.1730 |
| 1.85 x10 ⁻³ | 0.1428 | 0.2154 | | 0.0725 | 80.8 | | 80.7 | 1.0010 | 0.1791 |
| 5.64 x10 ⁻³ | 0.1235 | 0.2016 | | 0.0781 | 10.5 | | 77.3 | 1.3590 | 0.1626 |
| 7.29 x10 ⁻³ | 0.1191 | 0.2208 | | 0.1017 | 55.2 | | 11.0 | 0.5019 | 0.1700 |
| 1.07 x10 ⁻³ | 0.0943 | 0.2253 | | 0.1310 | 60.4 | | 10.6 | 0.5705 | 0.1597 |
| Da x10 ⁵ cm ² .s ⁻¹ | Dc x10 ⁵ cm ² .s ⁻¹ | <i>E</i> pc/2 | <i>E</i> pa- <i>E</i> pc/2 | Kscx10 ² | Fc x10 ⁹ mol.cm ⁻² | (+) | Qex10 ⁵ C | Γa x10 ⁹ mol.cm ⁻² | (-) <i>Q</i> a x10 ⁵ C |
| 1.7894 | 2.96 | 0.1551 | 0.0551 | 4.22 | 1.3662 | 1.66 | 5 | 1.0623 | 1.29 |
| 4.5547 | 4.54 | 0.1627 | 0.0526 | 4.93 | 1.6773 | 2.03 | 3 | 1.6791 | 2.03 |
| 8.3236 | 4.51 | 0.1570 | 0.0446 | 6.65 | 1.6058 | 1.95 | 5 | 2.1823 | 2.64 |
| 2.3845 | 9.47 | 0.1603 | 0.0605 | 2.12 | 2.2865 | 2.77 | 7 | 1.1476 | 1.39 |
| 3.0725 | 9.44 | 0.1673 | 0.0579 | 6.90 | 2.1999 | 2.67 | 7 | 1.2551 | 1.52 |

Table 3 focuses on the second redox transition in the system, likely corresponding to U(V)/U(IV). The shift in Ep,a and Ep,c values and the changes in Δ Ep further support the hypothesis that different uranyl species (e.g., UO_2 (OH)₄ $^{2-}$, UO_3 (OH)₃ $^{3-}$) are involved in complexation. As with the first redox couple, the increasing

Ip,a and Ip,c values confirm that higher paracetamol concentrations lead to greater redox activity. The formal potential (E°) values suggest a shift toward more favourable redox transitions.

Elevated diffusion coefficients indicate improved ion transport and stability of the complex species. The standard rate constant (ks) and transfer coefficient (α na) again reflect better electron exchange efficiency in the presence of paracetamol. Surface coverage (Γ a and Γ c) and charge passed (Qa and Qc) parameters further support this behaviour, showing higher adsorption of the active species and stronger electrochemical response. The second redox wave thus confirms a two-step interaction mechanism where paracetamol plays a stabilizing role across multiple oxidation states of uranium.

In summary, paracetamol acts as an effective chelating agent, significantly enhancing the redox behavior of uranyl ions in alkaline media. The observed shifts in peak positions, increased diffusion coefficients, and elevated charge transfer values substantiate the formation of uranyl-paracetamol complexes with improved electrochemical characteristics.

3.4. Stability Constants of Uranyl-Paracetamol Complexes

The stability constants (β_1) for uranyl–paracetamol interactions were determined via cyclic voltammetry by analysing the anodic peak potential shifts observed in the presence of paracetamol. These constants, which reflect the strength of interaction between the uranyl ion ($UO_2^{2^+}$) and paracetamol in alkaline medium (0.1 M NaOH), were evaluated from two prominent redox waves and are presented in **Table 4** [28-29]. No precipitation was observed during the experiments, indicating the formation of soluble hydroxylated uranyl–paracetamol complexes under the studied conditions. The changes in anodic peak potential ($E_{p,a}$) for the free uranyl ion and its complex form enabled the estimation of the stability constants (log β_1), which describe the equilibrium of complex formation between uranyl ions and paracetamol.

Table 4. Stability Constants and Thermodynamic Parameters for Uranyl-Paracetamol Complexes

| | Wave 1 | | | | | | | | | | | | |
|------------------------|------------------|---------|------------------------|---------|------------------------------|-------------|--------------------|--|--|--|--|--|--|
| [L] | Metal | Complex | $\Delta E \mathrm{mV}$ | log[I] | log P | D | A C (V I/mal) | | | | | | |
| mol.L ⁻¹ | (Ep,a)M | (Ep,a)C | | log[L] | $\log oldsymbol{eta_{j}}$ | $B_{\rm j}$ | $\Delta G(KJ/mol)$ | | | | | | |
| 9.35 x10 ⁻³ | 0.3558 | 0.1615 | 0.1943 | 4.0293 | 20.1783 | 1.5077 | -112.874 | | | | | | |
| 1.85 x10 ⁻³ | 0.3558 | 0.0848 | 0.2710 | 3.7323 | 28.1785 | 1.5084 | -157.626 | | | | | | |
| 5.64 x10 ⁻³ | 0.3558 | 0.1274 | 0.2284 | 3.2488 | 23.9881 | 9.7304 | -134.185 | | | | | | |
| 7.29 x10 ⁻³ | 0.3558 | 0.1516 | 0.2042 | 3.1373 | 21.5737 | 3.7473 | -120.679 | | | | | | |
| 1.07 x10 ⁻³ | 0.3558 | 0.1311 | 0.2247 | 2.9716 | 23.8850 | 7.6748 | -133.609 | | | | | | |
| | | | Wa | ve 2 | | | | | | | | | |
| [L] | Metal | Complex | $\Delta E \mathrm{mV}$ | log[I] | log R | D | ∆G(KJ/mol) | | | | | | |
| mol.L ⁻¹ | (<i>E</i> p,a)M | (Ep,a)C | | log[L] | $\log oldsymbol{eta}_{ m j}$ | $B_{\rm j}$ | ΔG (KJ/III01) | | | | | | |
| 9.35 x10 ⁻³ | 0.3558 | 0.1730 | 0.1824 | 7.0293 | 12.7325 | 5.4017 | -71.2237 | | | | | | |
| 1.85 x10 ⁻³ | 0.3558 | 0.1791 | 0.1767 | 6.7323 | 12.4167 | 2.6107 | -69.4573 | | | | | | |
| 5.64 x10 ⁻³ | 0.3558 | 0.1626 | 0.1932 | 6.2488 | 13.9942 | 9.8691 | -78.2817 | | | | | | |
| 7.29 x10 ⁻³ | 0.3558 | 0.1700 | 0.1858 | 6.1373 | 13.6774 | 4.7577 | -76.5091 | | | | | | |
| 1.07 x10 ⁻³ | 0.3558 | 0.1597 | 0.1960 | 5.9716 | 12.2686 | 5.3872 | -68.6287 | | | | | | |

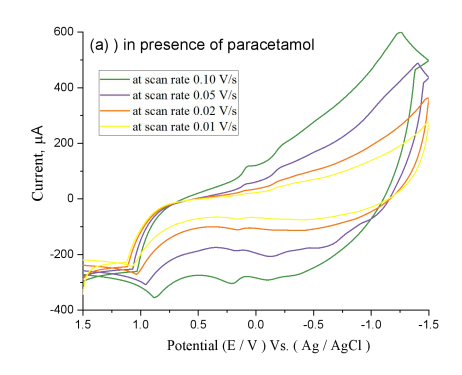
Table 4 presents the calculated stability constants (log β j) and Gibbs free energy (Δ G) values derived from cyclic voltammetry for two distinct redox waves. The shift in anodic peak potential (Ep,a) between free uranyl and the complex (Δ E) provides a quantitative basis for calculating log β j. Higher log β j values indicate stronger complex formation between uranyl ions and paracetamol, with values ranging from 12 to 28. The Δ G values are consistently negative, confirming the spontaneous nature of the complexation process. The stronger binding observed in Wave 1 (U⁶ $^+$) compared to Wave 2 (U⁴ $^+$) reflects the higher affinity of paracetamol toward the oxidized form of uranyl, possibly due to stronger electrostatic interactions. This thermodynamic analysis supports the kinetic data and validates the formation of a stable, soluble uranyl–paracetamol complex in alkaline medium. These findings reinforce the potential of paracetamol as a chelating and stabilizing agent for uranium ions in environmental or analytical applications.

The data reveal that higher $\log \beta_{\rm J}$ values correspond to stronger complex formation, with values ranging from approximately 12 to 28. All values of Gibbs free energy (ΔG) are negative, indicating that the complex reactions are spontaneous and thermodynamically favorable. These findings highlight the strong affinity between uranyl ions and paracetamol in alkaline media, consistent with the formation of stable coordination complexes.

Importantly, the stability of these complexes suggests that paracetamol could serve as an effective chelating agent for uranyl ions, with potential applications in uranium stabilization and nuclear waste remediation.

3.4. Effect of Scan Rate on the Redox Behavior of Uranyl Ions in the Presence and Absence of Paracetamol

To investigate the influence of scan rate on the electrochemical behavior of uranyl ions, cyclic voltammetry was performed in 0.1 M NaOH both with and without paracetamol (0.01 M) at varying scan rates. The results are depicted in Fig. 5.



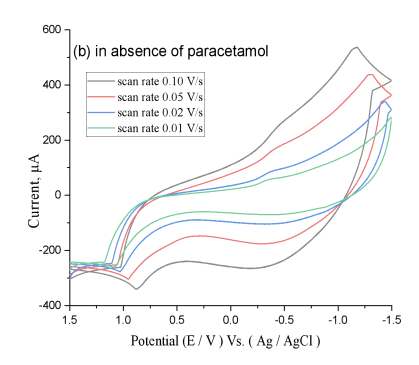


Fig. 5. Effect of Scan Rate

- (a) Cyclic voltammograms of uranyl nitrate (0.01 M) with paracetamol (0.01 M) in 0.1 M NaOH at various scan rates. Shows diffusion-controlled redox behaviour. Temperature: 298.15 K.
- (b) Cyclic voltammograms of uranyl nitrate (0.01 M) in 0.1 M NaOH at varying scan rates without paracetamol. Lower peak intensities observed. Temperature: 298.15 K.

The voltammograms reveal that in both cases, the redox processes are diffusion-controlled, as evidenced by the linear relationship between peak current and the square root of the scan rate. However, notable differences arise due to the presence of paracetamol. When paracetamol is present (Fig. 5a), there is a noticeable increase in peak current and a shift in peak potentials, indicating enhanced electron transfer kinetics and stronger redox activity[30–34].

In the absence of paracetamol (Fig. 5b), similar redox behaviour is observed, but with significantly lower peak currents. This contrast highlights the role of paracetamol in facilitating uranyl ion reduction and oxidation by forming electroactive complexes.

Cathodic peaks: With increasing scan rate, the peak potentials shift to more negative values, consistent with a diffusion-controlled process where the electron transfer rate is limited by the diffusion of the electroactive species to the electrode surface.

Anodic peaks: In contrast, anodic peak potentials shift towards more positive values with an increasing scan rate, also supporting diffusion control. The reversible redox behaviour further confirms the formation of stable uranyl-paracetamol complexes.

These results demonstrate that paracetamol enhances both the thermodynamic and kinetic aspects of uranyl ion redox behaviour. In alkaline conditions, paracetamol deprotonates and forms anionic species capable of chelating U(VI), thereby lowering the Gibbs free energy of solvation and facilitating redox transitions.

The electrochemical and thermodynamic insights gained from this study provide a foundation for developing treatment strategies involving organic chelators such as paracetamol. Moreover, the presence of such organic compounds should be carefully considered in the analysis of uranium speciation in environmental and industrial systems, as they may significantly alter both redox potential and complexation behaviour [35–42].

3.5. Molecular Docking Studies of Paracetamol and Its Uranyl Complex with Viral and Cancer-Related Proteins

To explore the potential biological relevance of paracetamol (PCM) and its uranyl complex beyond their conventional pharmacological applications, molecular docking simulations were conducted against selected viral and cancer-related protein

targets. These included the SARS-CoV-2 main protease (PDB ID: 7JWY) and a melanoma-associated antigen (PDB ID: 5IXB). The 7JWY target was selected due to its critical role in viral replication and relevance to the COVID-19 pandemic, while 5IXB represents a cancer-associated protein implicated in immune recognition of melanoma cells [43–46].

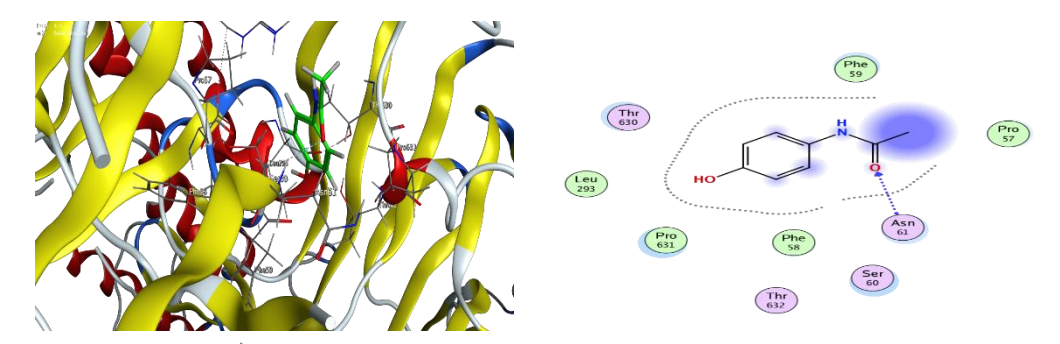
Specifically, 7JWY corresponds to the SARS-CoV-2 main protease (Mpro), a critical enzyme involved in viral replication. Given the global impact of COVID-19, this protein was chosen to explore the theoretical potential of paracetamol to interact with key viral targets, albeit only through silicon docking as a proof-concept without therapeutic claims.

On the other hand, 5IXB is a melanoma-associated antigen recognized by T cells. It was selected to assess paracetamol's theoretical binding affinity to cancer-related proteins, which complements literature suggesting paracetamol may modulate oxidative stress and inflammation—pathways often linked to tumor progression. While paracetamol is not an anticancer drug, exploring its binding affinity to this protein offers hypothetical biomedical insights that may inspire future studies.

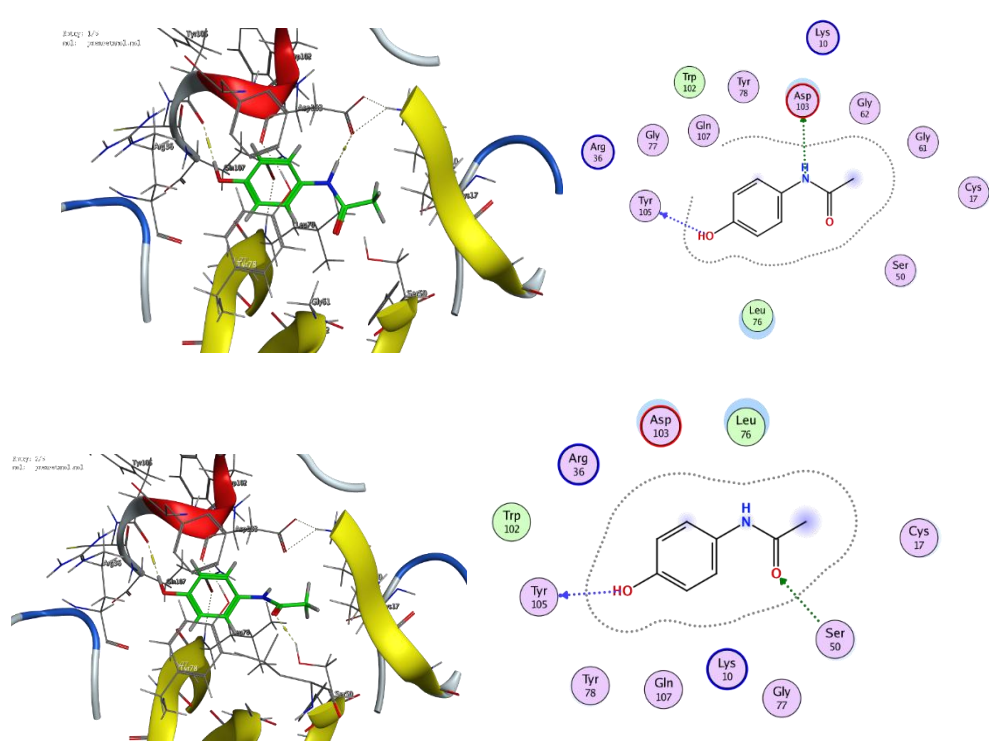
Docking studies were performed using the Molecular Operating Environment (MOE 2015.10). Ligands were geometry-optimized, and proteins were preprocessed by removing crystallographic water, adding hydrogens, and correcting protonation states at pH 7.4. A flexible ligand—rigid receptor approach was applied, and interaction parameters were evaluated for both hydrogen bonding and energetic favorability.

3.5.1. Docking of Free Paracetamol with 7JWY and 5IXB

The docking interactions of paracetamol with both viral and cancer proteins are summarized in **Table 5**, highlighting the key binding parameters, interaction types, and their potential implications. The 2D and 3D interaction models are illustrated in Fig. 6, visually representing the molecular binding sites and orientations.



a) Interaction of paracetamol with 7JWY viral protein for COVID-19



b) Interaction of paracetamol with Melanoma (eye cancer) protein 5IXB.

Fig. 6. Molecular docking of paracetamol

(a) 2D/3D interaction plot showing paracetamol docked to COVID-19 viral protein (PDB: 7JWY). (b) 2D/3D interaction plot showing paracetamol docked to melanoma-associated protein (PDB: 5IXB).

The 2D and 3D models depict binding sites, hydrogen bonds, and interaction distances, highlighting potential pharmacological implications. (a) COVID-19 protein 7JWY: Weak interaction (-1.1 kcal/mol) via hydrogen bonding with ASN-61 (3.07 Å) suggests limited but favourable interaction, potentially relevant for inflammation modulation during viral infections. (b) Melanoma protein 5IXB: Stronger binding (-3.1 kcal/mol) with TYR-105 (2.84 Å) and ASP-103 (3.17 Å), suggesting potential anticancer applications. Energy values are detailed in **Table 5**.

| Table 5. Molecular Docking Parameters of Paracetamol with SARS-CoV-2 | (7JWY |) and Melanoma (5 | 5IXB) Proteins |
|--|-------|-------------------|----------------|
|--|-------|-------------------|----------------|

| Ligand | Target | Interaction | Interaction | Distance | Binding | |
|-------------|----------|--------------|-------------|----------|------------|-------------------------|
| | Protein | Residue | Type | (Å) | Energy | Potential Implication |
| | | | | | (kcal/mol) | |
| Paracetamol | COVID-19 | N ASN 61 | H-bond | 3.07 | -1.1 | Weak interaction, |
| O 16 | (7JWY) | (H-acceptor) | (acceptor) | | | minimal antiviral |
| | | | | | | effect |
| Paracetamol | Melanoma | OD1 ASP | H-bond | 3.17 | -1.0 | Additional |
| N 11 | (5IXB) | 103 | (donor) | | | stabilization, moderate |
| | | (H-donor) | | | | binding affinity |
| Paracetamol | Melanoma | O TYR 105 | H-bond | 2.84 | -3.1 | Stronger interaction, |
| O 13 | (5IXB) | (H-donor) | (donor) | | | possible influence on |
| | | | | | | tumor progression |

For COVID-19 (7JWY): The binding energy of -1.1 kcal/mol suggests a weak but favourable interaction between paracetamol and COVID-19 protein (7JWY). The interaction distance of 3.07 Å indicates a moderate binding affinity, which could influence the protein's function. The binding involves hydrogen bond formation between paracetamol's oxygen and the ASN-61 residue of the viral protein, stabilizing the complex.

For Melanoma (5IXB): The binding energy of -3.1 kcal/mol suggests a stronger interaction with melanoma protein compared to COVID-19 protein. The shorter interaction distance (2.84 Å) with TYR 105 indicates a high affinity binding site, potentially influencing melanoma protein activity. Additional interaction with ASP 103 further supports the stabilization of the complex.

3.5.2. Energy Profile and Stability Analysis

To further assess the binding strength and conformational stability of the ligand–protein complexes, an in-depth energy decomposition analysis was conducted. The docking energy components are summarized in **Table 6**, which include conformation energy (E_{conf}), placement energy (E_{place}), scoring functions (E_{score1} and E_{score2}), and refinement energy (E_{refine}). To further understand the stability and strength of these molecular interactions, an energy profile analysis was performed for both viral and cancer protein docking. The docking energy values, as detailed in Table 6, highlight key energy components that determine the stability and feasibility of the paracetamol-protein complexes.

Table 6. Energy Profile of Paracetamol-Protein Docking Interactions

| Target Protein | Position | RMSD | $E_{ m conf}$ | E place | E score1 | E refine | E score2 |
|-----------------|----------|--------|---------------|----------|----------|----------|----------|
| COVID-19 (7JWY) | 1 | - | -4.2664 | -70.972 | -46.4583 | -18.4131 | - |
| | 2 | - | -3.9847 | -70.874 | -36.7277 | -16.3019 | - |
| Melanoma (5IXB) | 1 | 0.6002 | -70.7387 | -50.7491 | -6.87632 | -27.6929 | -5.5784 |
| | 2 | 1.5072 | -70.8549 | -34.864 | -6.55831 | -24.4986 | -5.3861 |

Interpretation of Energy Parameters:

- E_{conf} (Conformation Energy): Indicates the intrinsic stability of the ligand in the docked pose.
- E place (Placement Energy): Reflects the efficiency of ligand positioning in the binding pocket.
- E_{score1} (Scoring Function 1): Estimates the ligand's binding affinity in the first evaluation step.
- E_{refine} (Refinement Energy): Captures energy changes from post-docking refinement.
- E_{score2} (Final Scoring Function): The final estimation of the binding strength.

The docking data supports that paracetamol forms weak but energetically favourable interactions with the COVID-19 protein (7JWY). Although the binding affinity is low (-1.1 kcal/mol), the interaction may still be relevant for understanding paracetamol's secondary roles, such as inflammation modulation during viral infections.

Conversely, a stronger and more stable interaction is observed with the melanoma protein (5IXB), as evidenced by a more negative binding energy (-3.1 kcal/mol) and shorter hydrogen bond distances. These findings suggest that paracetamol may have unexplored implications in cancer biology, potentially influencing tumour progression pathways [47–50].

3.5.2. Docking of the Paracetamol-Uranyl Complex with SARS-CoV-2 Protein

To further evaluate how metal complexation alters the interaction profile of paracetamol, its 1:1 complex with uranyl ion (UO₂ ^{2*}) was subjected to docking with the SARS-CoV-2 main protease (7JWY). The metal-ligand complex was energy-minimized and docked using identical protocol parameters. The 2D and 3D interaction models are illustrated in Fig. 7, visually representing the molecular binding sites and orientations.

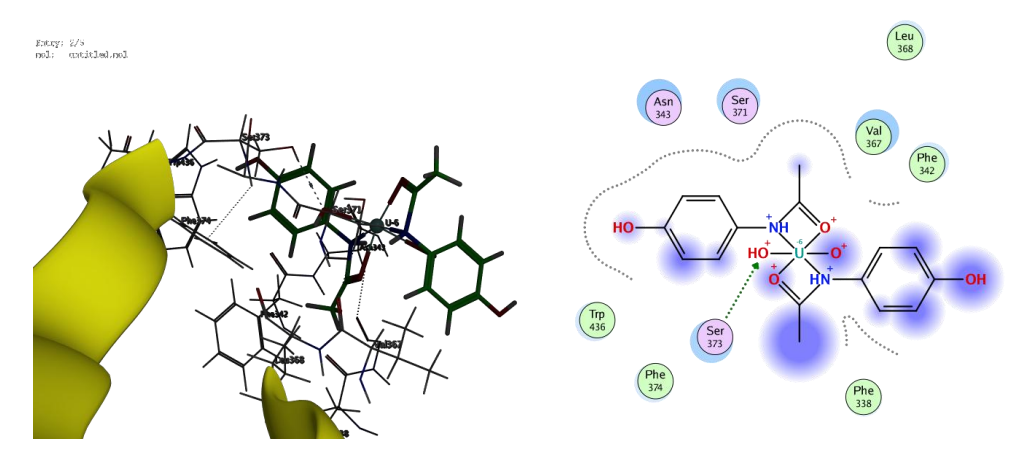


Fig. 7. Molecular docking of paracetamol-uranyl complex

2D/3D interaction plot showing paracetamol-uranyl complex docked to COVID-19 viral protein (PDB: 7JWY).

Energy values are detailed in **Table 7**. A hydrogen bond was observed between the O3 atom of the complex and SER-373 (OG) in the receptor's active site, with a bond distance of 2.98 Å and an interaction energy of -1.3 kcal/mol. Although this is only marginally stronger than the interaction with the free ligand, the incorporation of the uranyl ion clearly altered the docking conformation and electrostatic surface complementarity.

Table 7. Molecular Docking Parameters of Paracetamol with SARS-CoV-2 (7JWY) and Melanoma (5IXB) Proteins

| Ligand | Target Protein | Interact Residue | | Interaction Type | Distance (Å) | Binding Energy (kcal/mol) | Potential Implication |
|--------------|-------------------|---------------------|-----|---------------------|-----------------|---------------------------------|---------------------------|
| Paracetamol- | COVID-19 | SER | 373 | H-bond | 2.98 | -1.3 | Slight enhancement due to |
| Uranyl (O3) | (7JWY) | (OG) | | (acceptor) | | | metal coordination |

Full docking energy profile is provided in **Table 8**.

Table 8. Docking Energy Profile for the Paracetamol-Uranyl Complex with 7JWY

| Target Protein | Position | RMSD | $E_{ m conf}$ | E place | E score1 | E refine | E score2 |
|-----------------|----------|------|---------------|---------|----------|----------|----------|
| COVID-19 (7JWY) | 1 | 3.47 | -1697.76 | -61.70 | -7.56 | -18.73 | -4.49 |

These values suggest stable positioning of the complex within the active site, despite a modest final binding energy. The highly negative conformational energy reflects the structural rigidity of the uranyl complex, while the refinement score suggests adequate pose optimization.

3.5.3. Biological Insights and Hypothetical Relevance

The results indicate that free paracetamol and its uranyl complex can form energetically favorable, albeit weak, interactions with the viral main protease. The paracetamol—uranyl complex displayed slightly enhanced affinity and altered binding geometry, possibly attributed to increased charge density and metal coordination capabilities. These findings propose that metal complexation may modulate the bio-interactive profile of small molecules like paracetamol.

In contrast, paracetamol exhibited stronger binding with the melanoma protein, suggesting potential utility in modulating cancer-related pathways such as oxidative stress or inflammatory signaling. Although these docking studies are theoretical

and require experimental validation, they offer meaningful insights into repurposing or enhancing known drugs via metal coordination strategies [51–54].

3.6. Comparison with Previous Studies:

Compared to earlier studies that investigated paracetamol's redox behaviour using spectrophotometric or voltammetric methods in the absence of metal ions, our findings reveal a distinct electrochemical profile upon complexation with uranyl ions. Previous research on metal–paracetamol interactions focused largely on transition metals like Cu(II), Fe(III), and Zn(II), where complex formation typically enhanced antioxidant or biological properties. However, the interaction of paracetamol with actinide ions, particularly uranyl, has been rarely addressed [55–58]. Our results demonstrate for the first time that uranyl–paracetamol complexation in alkaline medium leads to measurable shifts in redox potentials and peak currents, confirming the formation of stable complexes. Additionally, the derived thermodynamic parameters (log β , ΔG) and the molecular docking with biologically relevant proteins distinguish this study by providing both chemical and theoretical insights not reported in earlier work[59–68].

4. Conclusions

This study demonstrated that paracetamol interacts electrochemically with uranyl ions in alkaline medium, forming stable complexes with observable shifts in redox peaks. The electrochemical parameters revealed diffusion-controlled, quasi-reversible behaviour with increased surface coverage and electron transfer efficiency. Calculated stability constants ($\log \beta$) and negative ΔG values confirm spontaneous complexation. Molecular docking showed paracetamol's moderate affinity for proteins 7JWY and 5IXB, suggesting theoretical biomedical relevance. The results indicate that free paracetamol and its uranyl complex can form energetically favorable, albeit weak, interactions with the viral main protease. The paracetamol—uranyl complex displayed slightly enhanced affinity and altered binding geometry, possibly attributed to increased charge density and metal coordination capabilities. These findings propose that metal complexation may modulate the bio-interactive profile of small molecules like paracetamol.

While promising, these in silico results require experimental validation. Overall, the integration of voltammetric and docking approaches offers a novel strategy for evaluating ligand–actinide interactions.

Although this study presents electrochemical and docking insights into paracetamol-uranyl interactions, the lack of experimental binding assays is a limitation. Future work should include such assays to validate and strengthen the theoretical findings.

In summary, this research illustrates the dual environmental and biomedical relevance of paracetamol. It establishes paracetamol as a promising molecule for future studies in redox chemistry, uranium sensing, and drug repurposing, particularly in oncology and virology contexts.

Interdisciplinary Relevance: The study bridges electrochemistry, environmental science, and molecular biology, offering valuable insights for researchers in these fields.

5. Conflicts of interest

There are no conflicts to declare.

6. Formation of funding sources

This research received no external funding.

References and Bibliography

- [1] Bouzidi M, Sellaoui L, Mohamed M, Franco DS, Erto A, Badawi M (2023) A comprehensive study on paracetamol and ibuprofen adsorption onto biomass-derived activated carbon through experimental and theoretical assessments. *Journal of Molecular Liquids* 376:121457
- [2] Mabrouk S, Fizer M, Mariychuk R, Dhaouadi H (2024) Grape seeds waste activated carbon as an adsorber of paracetamol drug residue: Experimental and theoretical approaches. *Journal of Molecular Liquids* **408**:125325
- [3] AbouElleef EM, Gomaa EA, Salem MA, Soud MR, El-Ghobashy MA (2024) Cyclic voltammetry analysis of mercuric chloride redox reactions with orange G dye. *Journal of Molecular Liquids* **415**:126171
- [4] AbouElleef EM, Gomaa EA, Salem MA, Soud MR, El-Ghobashy MA (2024) Conductometric study of hydroelectrochemical parameters for the interaction of cadmium bromide in lump and nano forms with Orange G dye. *Microchemical Journal* 196:109624
- [5] AbouElleef EM, Salem MA, Soud MR, Gomaa EA, El-Ghobashy MA (2023) Association thermodynamics parameters of nano vanadyl sulphate and its complexes with Orange G at different temperatures, docking versus Covid-19 and antioxidant behavior. *Journal of Molecular Liquids* **389**:122810
- [6] Alayyafi AA, Nasef HA, Salem SE, Gomaa EA, AbouElleef EM (2024) Effect of indomethacin on the electrical conductance and electrochemical voltammetry of copper chloride in methanol, ethanol, and their binary mixture with water. *Heliyon* 10(2):e24071

- [7] Abou Elleef EM, Abd El-Hady MN, Gomaa EA, Al-Harazie AG (2021) Conductometric association parameters for CdBr₂ in the presence and absence of Ceftazidime in water and 30% ethanol-water mixtures. *J Chem Eng Data* 66:878–889
- [8] Gomaa EA, Abou Elleef EM (2014) Thermodynamics of solvation of barium diphenylaminesulfonate in ethanol—water mixed solvents. *Thermal Power Eng* 3:222–226
- [9] Helmy ET, Gomaa EA, Abou Elleef EM (2016) Gibbs free energy and activation free energy of complexation of some divalent cations with ampicillin in methanol at different temperatures. *Am J Appl Chem* 4(6):256–259
- [10] Elgushe SM, El-Sonbati AZ, Diab MA, Gomaa EA, AbouElleef EM (2024) Eugenol's electrochemical behavior, complexation interaction with copper chloride, antioxidant activity, and potential drug molecular docking application for COVID-19. Colloids Surf B Biointerfaces 114194
- [11] Mishra S, Sini K, Jagadeeswara Rao Ch, Mallika C, Kamachi Mudali U (2016) Electrochemical studies on the reduction of uranyl ions in nitric acid–hydrazine media. *J Electroanal Chem* 776:127–133
- [12] Nazir M, Naqvi II (2013) Synthesis, spectral and electrochemical studies of complex of uranium(IV) with pyridine-3-carboxylic acid. Am J Anal Chem 4(3):7 pages. https://doi.org/10.4236/ajac.2013.43019
- [13] Moll H, Rosenberg A, Steudtner R, Drobot B, Muller K, Tsushima S (2014) Uranium(VI) chemistry in strong alkaline solutions. *Inorg Chem* 53:1585–1593
- [14] Islam MA, Nazal MK, Sajid M, Suliman MA (2024) Adsorptive removal of paracetamol from aqueous media: a comprehensive review of adsorbent materials, adsorption mechanisms, recent advancements, and future perspectives. J Mol Liq 123976
- [15] Wang Y, Hu B, Li Q, Wu Y, Shang X, Yang P, Feng W (2022) Novel phenanthroline-derived pyrrolidone ligands for efficient uranium separation: liquid–liquid extraction, spectroscopy, and molecular simulations. *J Mol Liq* 364:119909
- [16] AL-Ayash, S. R., & AL-Noor, T. H. (2022). A Review: Synthesis and characterization of metals complexes with paracetamol drug. *Analytical Science and Technology*, *35*(4), 143-152.
- [17] Aziz, A. A., Raoof, S. A., Hasan, W. M., & Saied, S. M. (2021). Preparation of New Complexes from a Mixture of Aspirin (acetylsalicylic acid), Paracetamol and Methyldopa with Divalent Manganese, Iron, Cobalt, Nickel and Copper, With a Study of Their Physical and Chemical Properties. *Egyptian journal of chemistry*, 64(5), 2405-2413.
- [18] Olanrewaju, A. A., Adeniyi, M. A., Oyebamiji, A. K., Oke, D. G., Adekunle, D. O., Akintelu, S. A., & Akinola, O. T. (2025). Preparation, characterization, antimicrobial evaluation, and molecular docking study of paracetamol and niacin mixed-drugs of Mn (II), Fe (II), and Co (II) complexes. *Discover Applied Sciences*, 7(3), 1-15.
- [19] Raoof, S. A., Hasan, W. M., Aziz, A. A., Saied, S. M., & Saleh, M. Y. (2022). Preparation of New Complexes of Bivalent Manganese, Iron, Cobalt, and Nickel with Mixed Ligands of Ciprofloxacin (Cip) and Metronidazole (Met) or 4-Aminoantipyrine (4AAP) with Study of Their Chemical, Physical Properties and Antibacterial Activity. *Egyptian Journal* of Chemistry, 65(9), 11-19.
- [20] Abou Elleef EM, Gomaa EA (2013) Thermodynamics of ion association in the saturated solution of barium diphenylamine sulfonate in ethanol–water mixed solvent. *Int J Eng Innov Technol (IJEIT)* 3(6):308–313
- [21] Hussein SQ, Gomaa EA, El-Defrawy MM, El-Ghalban MG, AbouElleef EM (2024) Study of the electrochemical properties of iron ions in various solutions including human blood using glassy carbon electrode and some theoretical applications. J Mol Liq 408:125366
- [22] Rashad RT, Nasef HA, Gomaa EA, AbouElleef EM (2024) Conductometric investigation of nano MnSO₄ association parameters and complex formation with glycylglycine in aqueous and methanol–water mixtures: thermodynamic parameters and potential applications. *Int J Biol Macromol* 267:131648
- [23] Wahba RH, El-Sonbati AZ, Diab MA, Gomaa EA, AbouElleef EM (2024) Electrochemical sensing of strontium ions by cyclic voltammetry and investigation of rosemary extract's effects on their behavior: antibacterial properties and molecular docking analysis for potential COVID-19 therapeutic benefits. *Microchem J* 200:110398
- [24] Abd El-Hady MN, Gomaa EA, Al-Harazie AG (2019) Cyclic voltammetry of bulk and nano CdCl₂ with ceftazidime drug and some DFT calculations. *J Mol Liq* 276:970–985
- [25] Al-Harazie AG, Gomaa EA, Zaky RR, Abd El-Hady MN (2024) Cyclic voltammetry studies of malonamide hydrazone derivative and its electrochemical effect on CdCl₂ . Electrochim Acta 476:143690
- [26] Wagman DD, Evans WH, Parker VB, Schumm RH, Halow I, Bailey SM, Nuttall RL (1989) Erratum: The NBS tables of chemical thermodynamic properties. Selected values for inorganic and C1 and C2 organic substances in SI units [J Phys Chem Ref Data 11 Suppl 2 (1982)]. J Phys Chem Ref Data 18(4):1807–1812
- [27] Wang P, Dong F, He D, Liu S, Chen N, Huo T (2021) Organic acid mediated photoelectrochemical reduction of U(VI) to U(IV) in wastewater: electrochemical parameters and spectroscopy. RSC Adv 11(38):23241–23248
- [28] Bansal NP, Plambeck JA (1981) Electroreduction of uranyl ion in aqueous calcium nitrate. Can J Chem 59:1515
- [29] Hussein SQ, El-Defrawy MM, Gomaa EA, El-Ghalban MG (2023) Analytical electrochemical sensing of calcium ions in HCl media in the presence of a dithizone ligand with its biological applications. *Int J Electrochem Sci* 18(9):100249
- [30] Gomaa EA, El-Sonbati AZ, Diab MA, El-Ghareib MS, Salama HM, et al. (2020) Cyclic voltammetry, kinetics, thermodynamic and molecular docking parameters for the interaction of nickel chloride with diphenylthiocarbazone. *Open Acad J Adv Sci Technol* 4:30–44
- [31] Hussien SQ, El-Defrawy MM, Gomaa EA, El-Ghalban MG (2024) Determination of calcium in water samples using Auelectrode in HCl solution in the absence and presence of crystal violet: environmental studies. *Bull Chem Soc Ethiop* 38(1):43–54
- [32] Resen ND, Gomaa EA, Salem SE, El-Defrawy AM, Abd El-Hady MN (2023) Cyclic voltammetry for interaction between mercuric chloride and diamond fuchsin (rosaniline) in 0.05 M NaClO₄ aqueous solutions at 303 K. Chem Methodol7:736-747

- [33] Ghandour MA, Abo-Doma RA, Gomaa EA (1982) Electroreduction (polarographically) of uranyl ion in nitric acid—methanol mixture media. *Electrochim Acta* 27:169–161
- [34] Gomaa EA, El-Defrawy MM, Hussien SQ (2020) Estimation of cyclic voltammetry data for SrCl₂ , CaCl₂ and their interaction with ceftriaxone sodium salt in KNO₃ using palladium working electrode. *Eur J Adv Chem Res* 1
- [35] AbouElleef EM, Gomaa EA, Mashaly MS (2018) Thermodynamic solvation parameters for saturated benzoic acid and some of its derivatives in binary mixtures of ethanol and water. J Biochem Technol 9(2):42–47
- [36] AbouElleef EM, Mekkey SD (2019) Study of the thermodynamic parameters for interaction of ciprofloxacin antibiotic with bulk and nanocopper sulfate. *J Biochem Technol* 10(1):57–66
- [37] Gomaa EA, AbouElleef EM, Helmy ET (2014) Solvation of oxytetracycline hydrochloride in ethanol–water mixed solvents. *Res Rev J Chem* 3(2):22–27
- [38] AbouElleef EM, Mahrouka MM, Salem SE (2021) A physical-chemical study of the interference of ceftriaxone antibiotic with copper chloride salt. *Bioinorg Chem Appl* 2021:4018843
- [39] Ahmadzadeh S, Yoosefian M, Rezayi M (2021) Comprehensive experimental and theoretical investigations on chromium(III) trace detection in biological and environmental samples using polymeric membrane sensor. *Int J Environ Anal Chem* 101(10):1461–1476
- [40] Rezayi M, Ahmadzadeh S, Kassim A, Lee Y (2011) Thermodynamic studies of complex formation between Co(Salen) ionophore with chromate(II) ions in AN-H₂ O binary solutions by the conductometric method. *Int J Electrochem Sci* 6:6350-6359
- [41] Ahmadzadeh S, Kassim A, Rezayi M, Rounaghi GH (2011) Thermodynamic study of the complexation of pisopropylcalix[6]arene with Cs⁺ cation in dimethylsulfoxide–acetonitrile binary media. *Molecules* 16(9):8130–8142
- [42] Ahmadzadeh S, Rezayi M, Karimi-Maleh H, Alias Y (2015) Conductometric measurements of complexation study between 4-isopropylcalix[4]arene and Cr³+ cation in THF–DMSO binary solvents. *Measurement* 70:214–224
- [43] Al-Nami SY, Aljuhani E, Althagafi I, Abumelha HM, Bawazeer TM, Al-Solimy AM, El-Metwaly N (2021) Synthesis and characterization of new nanometer Cu(II) complexes, conformational study and molecular docking approach compatible with promising in vitro screening. *Arab J Sci Eng* 46:365–382
- [44] El-Remaily MA, Soliman AM, Khalifa ME, El-Metwaly NM, Alsoliemy A, El-Dabea T, Abu-Dief AM (2022) Rapid, highly yielded and green synthesis of dihydrotetrazolo[1,5-a]pyrimidine derivatives in aqueous media using recoverable Pd(II) thiazole catalyst accelerated by ultrasound: computational studies. *Appl Organomet Chem* 36(2):e6320
- [45] El-Metwally NM, Arafa R, El-Ayaan U (2014) Molecular modeling, spectral, and biological studies of 4-formylpyridine-4 N-(2-pyridyl) thiosemicarbazone (HFPTS) and its Mn(II), Fe(III), Co(II), Ni(II), Cu(II), Cd(II), Hg(II), and UO₂ (II) complexes. *J Therm Anal Calorim* 115:2357–2367
- [46] Mohamed, A. A., El-Sherif, R., Mahmoud, W. H., & El-Sherif, A. A. (2025). Synthesis, Characterization, and Multifaceted Applications of Co (II) and Cu (II) Hydrazono Schiff Base Complexes: Integrating DFT, Molecular Docking, Biomedical Studies, and Nanotechnology-Enhanced Cadmium Detection Using Hydrazono Copper Complex-Based QCM. Egyptian Journal of Chemistry, 68(2), 537-560.
- [47] Nageeb, A. S., Morsi, M. A., Gomaa, E. A., Hammouda, M. M., & Zaky, R. R. (2024). Comparison on biological inspection, optimization, cyclic voltammetry, and molecular docking evaluation of novel bivalent transition metal chelates of Schiff Base pincer ligand. Journal of Molecular Structure, 1300, 137281.
- [48] Abid, M. N., Hafith, F. R., Musa, T. M., & Abbas, B. F. (2021). Synthesis, Characterization and Biological Activity Study of Cobalt (II), Nickel (II) and Copper (II) Complexes Derived from Mixed Bi dentate Ligands of Oxime and Phenanthroline. *Egyptian Journal of Chemistry*, 64(11), 6487-6492.
- [49] El-Gamasy, S. M., & Ebrahim, S. (2021). 4N donor atoms moiety of transition metal complexes of a Schiff base ligand: Synthesis, characterization and biological activities study. *Egyptian Journal of Chemistry*, *64*(10), 5975-5987.
- [50] Saleh, M. Y. (2022). Synthesis, characterization and biological evaluation study of cephalexin (Ceph) and Isatin Schiff base and its complexation with some divalent metal ions. *Egyptian Journal of Chemistry*, 65(7), 595-603.
- [51] Munshi, A. M., Bayazeed, A. A., Abualnaja, M., Morad, M., Alzahrani, S., Alkhatib, F., ... & El-Metwaly, N. M. (2021). Ball-milling synthesis technique for Cu (II)-Schiff base complexes with variable anions; characterization, potentiometric study and in-vitro assay confirmed by in-silico method. *Inorganic Chemistry Communications*, 127, 108542.
- [52] Katouah, H., Sayqal, A., Al-Solimy, A. M., Abumelha, H. M., Shah, R., Alkhatib, F., ... & El-Metwaly, N. M. (2020). Facile synthesis and deliberate characterization for new hydrazide complexes; cyclic voltammetry, crystal packing, eukaryotic DNA degradation and in-silico studies. *Journal of Molecular Liquids*, 320, 114380.
- [53] Abozeid, S. M., Snyder, E. M., Lopez, A. P., Steuerwald, C. M., Sylvester, E., Ibrahim, K. M., ... & Morrow, J. R. (2018). Nickel (II) complexes as paramagnetic shift and paraCEST agents. *European Journal of Inorganic Chemistry*, 2018(18), 1902-1908.
- [54] Fekri, A., & Zaky, R. (2016). Solvent-free synthesis and computational studies of transition metal complexes of the aceto-and thioaceto-acetanilide derivatives. *Journal of Organometallic Chemistry*, 818, 15-27.
- [55] Abbas, R. F., Allawi, A. G., Abdulhassan, N. M., & Mahmoud, N. H. (2020). Spectrophotometric Determination of Paracetamol using a Newly Synthesized Chromogenic Reagent 4-[(2-amino-1, 3thiazol-4-yl) amino] nitro benzene. *Egyptian Journal of Chemistry*, 63(12), 4681-4693.
- [56] Al-Niemi, H., & Mahmoud, M. (2023). Kinetic Study for the reactions of paracetamol with diazotized (P-nitroaniline & sulfanilic acid sodium salt) reagents. *Egyptian Journal of Chemistry*, 66(2), 535-542.

- [57] Hussein, L. M., Badawy, M. A., Gad, S. S., & Abd EL-Rahman, H. A. (2025). The prospective impact of paracetamol medication on female Wistar rats' reproductive health (biochemical, genotoxic, and histological analysis). *Egyptian Journal of Chemistry*, 68(9), 1-16.
- [58] Mukui, A. M., Bishi, A. A., Ghazwani, B. H. A., Alnasyan, T. M., Alkhaibari, B. N., Sharahili, A. Y., ... & Alkhybari, N. A. (2025). An Updated Review About Pain Management Medications and Biochemical Mechanisms-Overview for Healthcare Professionals. *Egyptian Journal of Chemistry*, 68(2), 135-144.
- [59] GOMAA, E. A., ABOU ELLEET, E. M., Helmy, E. T., & DEFRAWY, S. M. (2013). SOLVENT EFFECTS ON THE THERMODYNAMICS OF SOLVATION OF BARIUUM DIPHENYLAMINESULFONATE IN ETHANOL-WATER MIXED SOLVENTS. SOUTHERN JOURNAL OF SCIENCES, 21(21), 31-40.
- [60] Abou Elleef, E. M., & Gomaa, E. A. (2013). Thermodynamics of Ion Association in the Saturated Solution of Barium Diphenyl amine sulfonate in Ethanol-Water Mixed Solvent. *International Journal of Engineering and Innovative Technology (IJEIT)*, 3(6), 308-313.
- [61] Wahba, R. H., El-Sonbati, A. Z., Diab, M. A., Gomaa, E. A., & AbouElleef, E. M. (2024). Electrochemical sensing of strontium ions cyclic voltammetry and investigation of rosemary extract's effects on their behavior: Antibacterial properties of rosemary extract and molecular docking analysis for potential COVID-19 therapeutic benefits. *Microchemical Journal*, 200, 110398.
- [62] Alayyafi, A. A., Ghanem, K. Z., Almarri, M. S., Salem, S. E., Gomaa, E. A., & AbouElleef, E. M. (2025). Conductometric, physico-chemical, and biological activity investigations of a copper-indometacin complex. *Green Chemistry Letters and Reviews*, 18(1), 2455938.
- [63] El-Zohiray, M. A. G., Gomaa, E. A., El-Defrawy, M. M., Abd El-Hady, M. N., & AbouElleef, E. M. (2025). Electrochemical Behavior and Complexation of Thallous Chloride in Aqueous Solutions: Insights from Cyclic Voltammetry with Bromocresol Green. *Journal of the Indian Chemical Society*, 101851.
- [64] AbouElleef, E. M., Saad, R. A., Diab, M. A., El-Zahed, M. M., El-Sonbati, A. Z., & Morgan, S. M. (2025). Synthesis, characterization, biological evaluation and molecular docking of a Schiff base ligand and its metal complexes. *BioMetals*, 1-29
- [65] Raoof, S. A., Hasan, W. M., Aziz, A. A., Saied, S. M., & Saleh, M. Y. (2022). Preparation of New Complexes of Bivalent Manganese, Iron, Cobalt, and Nickel with Mixed Ligands of Ciprofloxacin (Cip) and Metronidazole (Met) or 4-Aminoantipyrine (4AAP) with Study of Their Chemical, Physical Properties and Antibacterial Activity. Egyptian Journal of Chemistry, 65(9), 11-19.
- [66] Abid, M. N., Hafith, F. R., Musa, T. M., & Abbas, B. F. (2021). Synthesis, Characterization and Biological Activity Study of Cobalt (II), Nickel (II) and Copper (II) Complexes Derived from Mixed Bi dentate Ligands of Oxime and Phenanthroline. Egyptian Journal of Chemistry, 64(11), 6487-6492.
- [67] El-Gamasy, S. M., & Ebrahim, S. (2021). 4N donor atoms moiety of transition metal complexes of a Schiff base ligand: Synthesis, characterization and biological activities study. Egyptian Journal of Chemistry, 64(10), 5975-5987.
- [68] Saleh, M. Y. (2022). Synthesis, characterization and biological evaluation study of cephalexin (Ceph) and Isatin Schiff base and its complexation with some divalent metal ions. Egyptian Journal of Chemistry, 65(7), 595-603.